Outflows, Edges & Wakes: Probing Galaxy Evolution with Chandra and XMM-Newton

M. Machacek, C. Jones, W. R. Forman, P. Nulsen, R. Kraft

Harvard-Smithsonian Center for Astrophysics

An array of physical processes, often acting in concert, affect the evolution of galaxies and the intracluster medium (ICM) in groups and clusters. These processes include tidal interactions from galaxy collisions and mergers, ram pressure and turbulent viscous stripping of galaxy gas caused by the galaxy's motion through the ambient group/cluster gas, and outflows induced by star formation and/or AGN activity powered by accretion onto a central black hole within the galaxy. Each process imprints characteristic signatures, such as cavities, surface brightness edges, and wakes, on the hot gas in and near the galaxy. We use Chandra and XMM-Newton X-ray observations of nearby galaxies, spanning a range of galaxy types and environments, including elliptical galaxies NGC 4552 in Virgo, NGC 7618 near the UGC 12491 group, NGC 7619 in Pegasus I, and the interacting pair NGC 4782/3, and spiral galaxies NGC 6872 in the Pavo group and NGC 2276 in the NGC 2300 group, to investigate the physical processes at work in the evolution of these systems.

ELLIPTICAL GALAXY NGC 4552 IN THE VIRGO CLUSTER

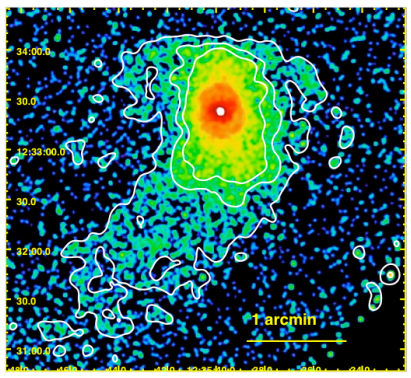

FIG. 1.— Chandra image of the 0.5 – 2 keV diffuse emission in NGC 4552 in the Virgo Cluster. Point sources have been removed and the image has been background subtracted, exposure corrected and smoothed with a Gaussian kernel with $\sigma = 1''$. Contours denote X-ray surface brightness levels of 0.4, 1, 2×10^{-8} photons s^{-1} cm^{-2} arcsec^{-2}, respectively. North is up and east is to the left.

In Fig. 1 we show the 0.5 – 2 keV diffuse emission, as measured in a 54 ks Chandra observation of the elliptical galaxy NGC 4552 in the Virgo Cluster (Machacek et al. 2005c). The 0.5 – 2 keV X-ray emission shows the classic features of ram pressure stripping, as found in simulations (e.g. see Stevens et al. 1999; Toniazzo & Schindler, 2001; Acreman et al. 2003), of a gas rich galaxy moving supersonically through the surrounding Virgo ICM. We see:

- a sharp, flattened leading surface brightness edge located 3.1 kpc from the center of NGC 4552 due to the ram-pressure of the Virgo ICM. The temperature of galaxy gas inside the leading edge is cool ($kT = 0.43^{+0.02}_{-0.033}$ keV), a factor ~ 5 lower than the surrounding 2.2 keV Virgo ICM, consistent with the leading edge being a "cold front" (Vikhlinin et al. 2001; Machacek et al. 2005a).
- two cool ($kT \sim 0.3 - 0.6$ keV) horns of emission extending 3 – 4 kpc to either side of the edge, consistent with galaxy gas in the process of being stripped due to the onset of Kelvin-Helmholtz instabilities, and
- a cool ($kT \sim 0.51^{+0.09}_{-0.08}$ keV), dense ($n \sim 5.4 \pm 1.7 \times 10^{-3}$ cm^{-3}) tail of emission extending ~ 10 kpc behind NGC 4552 opposite the leading edge.

Following Viklinin et al. (2001), we use the pressure ratio between gas inside the cold front and the free-streaming Virgo ICM to constrain the three dimensional motion of NGC 4552 relative to the Virgo ICM. Assuming that NGC 4552 and M87 (Virgo Cluster center) both lie in the plane of the sky, we combine our spectral data with fits to the surface brightness profile, as shown in Fig. 2 below, and find density and pressure ratios between gas inside the cold front and the free streaming Virgo ICM of 35 ± 7 and $\sim 7 \pm 1.4$, respectively. These results suggest that NGC 4552 is moving at Mach 2.1 ± 0.2 through the cluster gas with speed $v \sim 1610 \pm 150$ km s^{-1} at an angle $\xi \sim 37^{\circ +5}_{-4}$ towards us with respect to the plane of the sky.

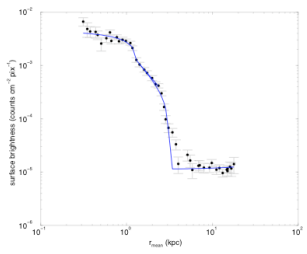

FIG. 2.— The 0.5 – 2 keV surface brightness profile as a function of distance from the center of NGC 4552 across the galaxy's leading edge to the north. The blue line denotes results for a simple power law density model with $n_e \propto r^{-\alpha}$ within the galaxy where $\alpha = -0.1^{+0.1}_{-0.25}$, inside the inner edge ($r < 1.3$ kpc) and $\alpha = 1.3 \pm 0.2$ between the two edges ($1.3 \leq r < 3.1$ kpc). For $r \geq 3.1$ kpc the Virgo ICM is modelled by a β model with $\beta = 0.47$ and core radius $r_c = 2'.7$ (Schindler et al. 1999).

Two ring-like emission features, consistent with bipolar nuclear outflow cavities, are found in the X-ray images at $r \sim 1.3$ kpc from NGC 4552's center (See Fig. 3 below).

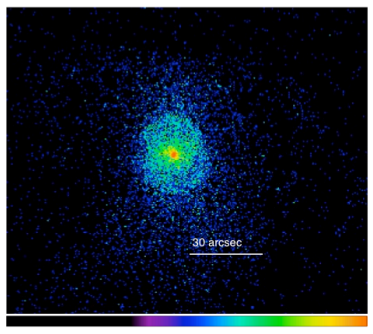

FIG. 3.— Chandra image of the 0.5 – 2 keV diffuse emission from the inner rings in the central region of NGC 4552.

In contrast to the cold front, the rise in surface brightness (and density) at the rims of the rings, shown at $r = 1.3$ kpc in Fig. 2, also corresponds to a rise in the temperature, $kT = 0.61 \pm 0.02$ keV, measured through the ring rims, consistent with the rings being shocks.

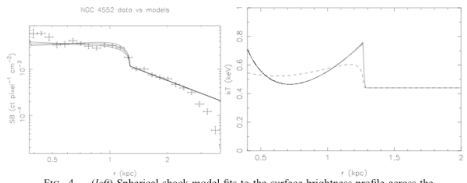

FIG. 4.— (*left*) Spherical shock model fits to the surface brightness profile across the inner edge for a preshocked isothermal (0.43 keV) $r^{-1.3}$ density distribution inside the galaxy. Upper, middle and lower lines represent shock Mach numbers 1.9, 1.7 and 1.6, respectively. (*right*) Temperature profile (solid line) for the Mach 1.7 model shock shown in the left panel. Dashed line denotes the emission-measure-weighted temperature profile for lines of sight through the galaxy.

Modeling these shocks with simple spherical models (Nulsen et al. 2005), as shown above in Fig. 4, the shape of the surface brightness profile across the rims and the temperature of the gas in the ring rims are consistent with a Mach 1.7 shock with mean mechanical power $L_{\rm mech} \sim 3 \times 10^{41}$ erg s^{-1} produced by a $\sim 1.4 \times 10^{55}$ erg nuclear outburst $\sim 1 - 2$ Myr ago. One outburst of this magnitude every ~ 18 Myr would be sufficient to balance the radiative cooling of the hot ISM in NGC 4552.

TRANSONIC INFALL OF ELLIPTICAL GALAXIES INTO GROUPS

The characteristic leading edge–trailing wake morphology in the X-ray surface brightness, suggestive of ram pressure and/or turbulent-viscous stripping of galaxy gas, is also seen in the subsonic/transonic infall of elliptical galaxies into groups.

NGC 7619 in Pegasus I

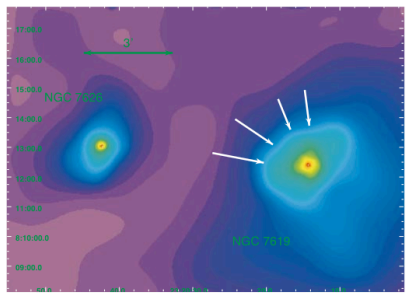

FIG. 5.— An adaptively smoothed, background subtracted, exposure corrected Chandra/ACIS-I image of NGC 7619 and NGC 7626, the two dominant elliptical galaxies of the Pegasus I group.

In Fig. 5 above we show a Chandra/ACIS-I image of NGC 7619 and NGC 7626, the two dominant elliptical galaxies in the Pegasus I group. In contrast to the transonic infall of elliptical galaxies in clusters, as in NGC 1404 falling towards NGC 1399 in Fornax where a factor $\sim 5 - 6$ rise in density is accompanied by a factor ~ 3 drop in temperature between the free-streaming ICM and galaxy gas inside the leading edge (Machacek et al. 2005a), there is no significant difference in the gas temperature across the discontinuity for NGC 7619. Fitting the surface brightness profile of NGC 7619 with simple density models, we do find a pressure jump of ~ 1.5 across the edge. From 2D hydrodynamical simulations of Mach 0.5 – 1.0 infall of galaxies into a group potential, we show such pressure discontinuities can be maintained in these flows when an equilibrium is established between the external ram pressure and the internal gas pressure and gravitational potential (Kraft et al. in preparation).

NGC 7618: Infall into a Failed Cluster?

The leading edge – trailing wake morphology is also seen in Fig. 6 in Chandra images of the elliptical galaxy NGC 7618, located $\sim 14'.1$ from galaxy group UGC 12491. These features could result from a radio lobe/IGM interaction, from a gravitational interaction with UGC 12491, from "sloshing" of gas in the larger scale dark matter halo due to a recent merger, or from ram-pressure stripping due to infall into a larger gravitational potential. Although deeper observations are needed to distinguish between these scenarios, ASCA/GIS observations of $\sim 3 - 4$ keV diffuse gas surrounding NGC 7618 suggest that the X-ray features in NGC 7618 are likely the result of ram-pressure stripping of group gas during either a group-group merger or infall of the two groups into a larger dark matter potential (Kraft et al. in preparation).

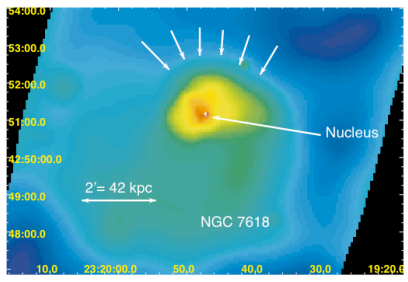

FIG. 6.— An adaptively smoothed, background subtracted, exposure corrected 0.5 – 2 keV Chandra/ACIS-S image of NGC 7618.

THE DUMBBELL GALAXIES: NGC 4782 (3C278) & NGC 4783

Dumbbell galaxy systems, such as NGC 4782 and NGC 4783, offer a unique window into the study of strongly interacting galaxies and their impact on their environment. NGC 4782/3 shows a $v > 700$ km s^{-1}, deeply penetrating encounter of two roughly equal mass elliptical galaxies, viewed 13.5 – 25 Myr after pericenter passage, and is likely the prelude to the galaxies' eventual merger (Borne et al. 1988; Madjesky & Bien 1993).

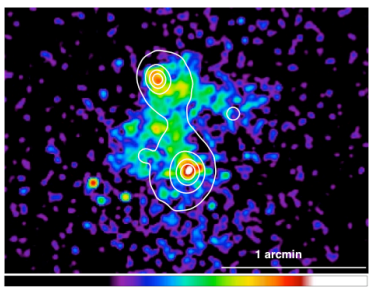

FIG. 7.— 0.3 – 2 keV Chandra X-ray image of the NGC 4782/3 dumbbell system overlaid with linearly spaced contours from the 2MASS J-band image of the system. NGC 4783 is to the north and NGC 4782 is to the south. The Chandra X-ray image has been background-subtracted, exposure corrected and smoothed with a $\sigma = 1''$ Gaussian kernel.

In Fig. 7 we overlay a 0.3 – 2 keV Chandra ACIS-S image of NGC 4782/3 with linearly spaced contours from the 2MASS J-band image of this system. We find (Machacek et al. in preparation):

- the peak of the X-ray emission in each galaxy is off-centered and coincident with the peak in the J-band isophotes of each galaxy. Instead of distorted stellar arms seen in tidally interacting spiral galaxies (see Fig. 10), the signature for tidal interactions between elliptical galaxies is such an off-centering of the optical isophotes (Borne et al. 1988).
- X-ray emission from surrounding hot group gas is observed to $> 5'$ from NGC 4782, with temperatures increasing from ~ 1 keV at large radii to 1.4 – 2 keV near the interacting system, suggesting the interaction is occuring near the core of a massive dark group halo.
- a sharp X-ray surface brightness discontinuity on the eastern edge of NGC 4783 (northern galaxy) with an extended trailing wake to the west, indicating NGC 4783 is moving to the east at high speed relative to the surrounding group gas. These features suggest that ram pressure and turbulent viscous stripping may also be important.
- the temperatures of gas in the galaxy features are cool, $\sim 0.5 - 6$ keV in the central regions of the galaxies and $\sim 0.6 - 0.8$ keV in the gas between and trailing each galaxy, consistent with galaxy gas ram-pressure and/or tidally stripped.

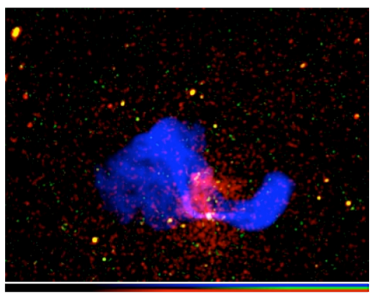

FIG. 8.— Tricolor image of NGC 4782/3 with the VLA image of 5 GHz radio emission in blue, and Chandra 0.3 – 2 keV and 2 – 8 keV images in red and green, respectively. The Chandra images have been background subtracted, exposure corrected and smoothed with a $\sigma = 1''$ Gaussian kernel.

NGC 4782 has long been known to host the strong radio source 3C278 (Harris & Roberts 1960). In Fig. 8 we show a VLA 5 GHz image (M. Hardcastle, private communication) of the twin radio jets (blue) from 3C278 superposed on the 0.3 – 2 kev (red) and 2 – 8 keV (green) Chandra X-ray images of NGC 4782/3. The asymmetric radio lobes carve out large X-ray cavities in the surrounding group IGM, and as shown in Fig. 9, X-ray knots (E1, W1, W2) are found in the Chandra images near the nucleus (N) of NGC 4782, coincident with the ends of highly collimated radio features in the jets.

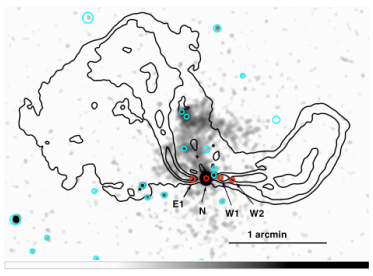

FIG. 9.— Chandra 0.3 – 2 keV X-ray image of NGC4782/3 (greyscale) overlaid with VLA 5 GHz radio contours and X-ray point sources identified in the Chandra images in the 0.3 – 8 keV bandpass. X-ray knots (E1, W1, W2), likely associated with the radio jet, and the nucleus (N) are shown in red.

SPIRAL GALAXY NGC 6872 IN PAVO

NGC 6872 in the Pavo Group, shown in Fig. 10, hosts a particularly intriguing array of galaxy-galaxy and galaxy-gas interactions in a cool group environment. This large spiral galaxy NGC 6872 shows dramatic evidence of tidal damage in its long, distorted stellar spiral arms. The path of a recent collision between NGC 6872 and nearby companion galaxy IC 4970 is traced by a stellar bridge connecting IC 4970 to NGC 6872's northern spiral arm.

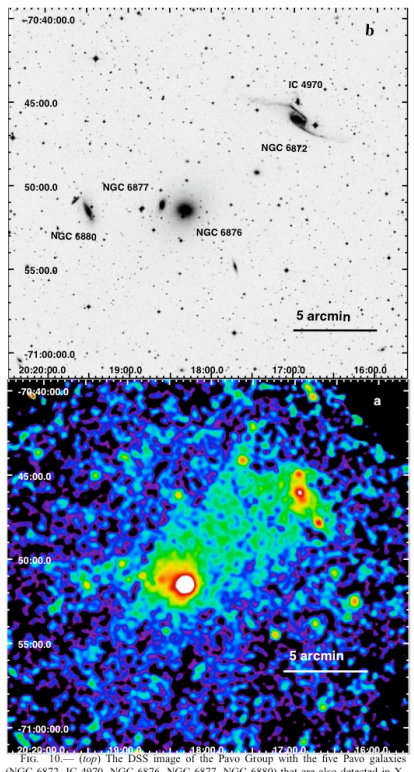

FIG. 10.— (*top*) The DSS image of the Pavo Group with the five Pavo galaxies (NGC 6872, IC 4970, NGC 6876, NGC 6877, NGC 6880) that are also detected in X-rays labeled. (*bottom*)The XMM-Newton 0.5 – 2 keV background-subtracted, exposure corrected, coadded MOS and PN images from a 32.2 ks XMM-Newton observation of the Pavo galaxy group. The trail (wake) of enhanced X-ray emission extending between the dominant elliptical NGC 6876 and the large spiral NGC 6872 is evidence of interaction between the spiral and the group.

Perhaps most surprising is our discovery, using XMM-Newton data, of a hot X-ray trail (see Fig. 10 lower panel) connecting, in projection, the large spiral NGC6872 to the dominant group elliptical NGC 6876 (Machacek et al. 2005b), and providing dramatic evidence for the interaction of the spiral NGC 6872 with the Pavo group. Results from our analysis of the X-ray trail are:

- the trail is long, spanning the full $\sim 67 \times 100$ kpc projected distance between NGC6876 and NGC6872;
- the temperature of the trail (~ 1 keV) is twice that of the ambient Pavo IGM;
- the mean density of the trail (9.5×10^{-3} cm^{-3}) is ~ 1.7 times larger than that of undisturbed Pavo group gas at the same mean distance from the group center;
- the geometry and physical properties of the trail strongly suggest that NGC 6872 is moving at $\gtrsim 1200$ km s^{-1} (Mach $\gtrsim 3$) through the densest regions of the Pavo IGM.

Although rare today, such high velocity interactions were likely common at high redshift, when the number densities of groups and subgroups undergoing collisions and mergers was greater.

Processes that could contribute to the formation of the X-ray trail are:

- Tidal stripping from either NGC6876 or NGC6872, during their close encounter near the deepest part of the group potential. Tidal interactions with the group or the spiral's companion IC 4970 may also enhance other gas stripping processes by moving ISM gas to a higher potential where it could be more easily stripped.
- Ram-pressure stripping (Gunn & Gott 1972) where ISM gas is bodily pushed out from the spiral NGC 6872 by the pressure of the Pavo IGM during the spiral's passage through the group IGM.
- Bondi-Hoyle gravitational focusing (Bondi 1952) of the IGM gas into a trailing wake by the dark matter halo of NGC6872 and IC4970, as the spiral-dominated subgroup passes through dense IGM near the Pavo group core.
- Turbulent viscous stripping (Nulsen 1982) of ISM gas from NGC6872, that is then thermally mixed with the ambient IGM gas.

The current data suggest that the long trail is most likely either a thermal mixture of $\sim 60\%$ Pavo IGM gas with $\sim 40\%$ galaxy gas that has been removed from the spiral NGC 6872 by turbulent viscous stripping, or IGM gas gravitationally focused into a Bondi-Hoyle wake, or both, due to the spiral's supersonic motion through the densest region of the Pavo IGM.

SPIRAL GALAXY NGC 2276 IN THE NGC 2300 GROUP

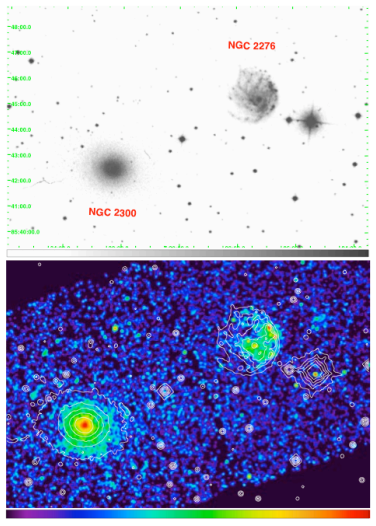

FIG. 11.— *top* DSS B-band image of the spiral galaxy NGC 2276 and the central group elliptical galaxy NGC 2300 in the NGC 2300 galaxy group. Note the sharp truncation of the stellar distribution and bow-shaped appearance of the western edge of NGC 2276. *bottom* 0.3 – 2 keV Chandra X-ray image overlaid with linearly spaced contours from the top image. The Chandra image has been background-subtracted, exposure corrected and smoothed with a $\sigma = 2''$ Gaussian kernel. Note the close correspondence of the 0.3 – 2 keV X-ray and optical emission in the spiral galaxy.

A second example of a large spiral galaxy in interaction with its environment is NGC 2276 in the poor NGC 2300 group. As shown in the top panel of Fig. 11, there is a sharp truncation of the stellar light along the western edge as compared to the east. This bow-shaped western morphology is also found in all tracers of the cool ISM (CO, Hα, HI, 20 cm radio continuum) with recent star formation clustered near the western edge. The disturbed morphology and enhanced star formation are likely the result of both a gravitational interaction of NGC 2276 with the central galaxy NGC 2300 or the core of the group potential and ram-pressure from NGC 2276's motion through the group IGM (Davis et al. 1997).

X-ray observations by ROSAT (Davis et al. 1997, Liu & Bregman 2005) and XMM-Newton (Davis & Mushotzky 2004) showed that the X-ray emission in NGC 2276 shares the same distorted morphology as the stars and cool ISM, with the peak X-ray emission displaced from the nucleus and located near the sharp western edge. This is confirmed by a 0.3 – 2 keV Chandra image overlaid with optical contours shown in the lower panel of Fig. 11. As shown in the high resolution Chandra image in Fig. 12, we find the peak of the X-ray emission dominated by 3 X-ray point sources along the western edge, that are likely associated with recent star formation triggered by the interactions.

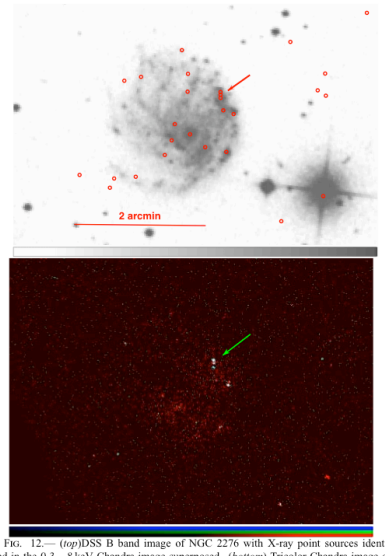

FIG. 12.— (*top*)DSS B band image of NGC 2276 with X-ray point sources identified in the 0.3 – 8 keV Chandra image superposed. (*bottom*) Tricolor Chandra image of NGC 2276 showing 0.3 – 1 keV (red), 1 – 2 keV (green) and 2 – 8 keV (blue) X-ray emission. Each pixel is $0.49'' \times 0.49''$.

Acknowledgements

This work was supported in part by the Smithsonian Institution, Chandra X-ray Center, and NASA grant GO3-4176A.

REFERENCES

Acreman, D et al. 2003, MNRAS, 341, 1333
Bondi, H. 1952, MNRAS, 112, 195B
Borne,K. et al. 1988, ApJ, 333, 567
Davis, D. et al. 1997, AJ, 114, 613
Davis, D. & Mushotzky, R. 2004, ApJ, 604, 653
Gunn, J. & Gott J., 1972, ApJ, 176, 1
Harris, D. & Roberts, J. 1960, PASP, 72, 237
Liu, J.-F. & Bregman, J. 2005, ApJS, 157, 59
Madejsky R. & Bien, R. 1993, A & A, 280, 383
Machacek, M. et al. 2005a, ApJ, 621, 663
Machacek, M. et al. 2005b, ApJ, 630, 280
Machacek, M. et al. 2005c, ApJ, submitted, eprint astro-ph/0508588
Nulsen, P.J.E. 1982, MNRAS, 198, 1007
Nulsen, P.J.E. 2005, ApJ, 628, 629
Schindler et al. 1999, A & A, 343, 420
Stevens et al. 1999, MNRAS, 310, 663
Toniazzo, T. & Schindler, S. 2001, MNRAS, 325, 509

Vikhlinin, A. et al. 2001, ApJ, 551, 160